GFD 2017 Lecture 5: Basic Theory of Ice-Ocean Interaction

Adrian Jenkins; notes by Madeleine Youngs and Guillaume Michel

June 23, 2017

In this lecture, we detail the structures of the ice-ocean boundary layers and of the water motion beneath an ice shelf. These flows strongly depend on the thermodynamic properties of water (*e.g.* latent heat, phase diagram, equation of state) and we therefore first review these properties of fresh and salty water before turning to fluid mechanics.

1 The Ice-ocean Interface and the Boundary Layer

1.1 Impact of the melting of ice on the ocean

1.1.1 Phase diagram of water

For a mixture of ice and fresh water to be at equilibrium, the temperature has to be equal to the freezing temperature T_f , which only depends on the pressure. At one atmosphere, this temperature is very close to 0°C, and (unlike most other pure substances) it *decreases* as the pressure increases, approximately as $-1 \times 10^6\,\mathrm{Pa}\cdot\mathrm{K}^{-1}$.

Because seawater contains ions, its thermodynamic properties also depend on the *salinity*. Once the pressure is fixed, the dependence of the freezing point on salinity can be seen on the phase diagram Fig. 1. For simplicity, we describe in the following a mixture of pure water and salt (NaCl).

In this figure, the grey zones are delimited by the *liquidus* (boundary with the liquid solution) and the *solidus* (boundary with the solid solution). If the temperature and salinity are set such that the system falls into one of these two grey zones, the equilibrium state is a coexistence between a liquid solution and a pure solid (either ice or salt). The point E is called an eutectic point, and corresponds, at one atmosphere, to a temperature of -21.2°C and a salinity per mass of 23.3%.

These coexistence zones are of importance for ice-ocean interfaces: the melting of pure ice in seawater tends to drive the liquid toward the liquidus. For instance, consider the total melting of a mass of ice ΔM (temperature T_i, salinity $S_\mathrm{i} = 0$) into a mass of seawater M (temperature T_w, salinity S_w). The final properties of the liquid (T_mix, S_mix) follow from the conservation of energy and mass. The first principle of thermodynamics reads

$$M c_\mathrm{w}(T_\mathrm{mix} - T_\mathrm{w}) + \Delta M\,[c_\mathrm{w}(T_\mathrm{mix} - T_\mathrm{f}) + \ell + c_\mathrm{i}(T_\mathrm{f} - T_\mathrm{i})] = 0, \tag{1}$$

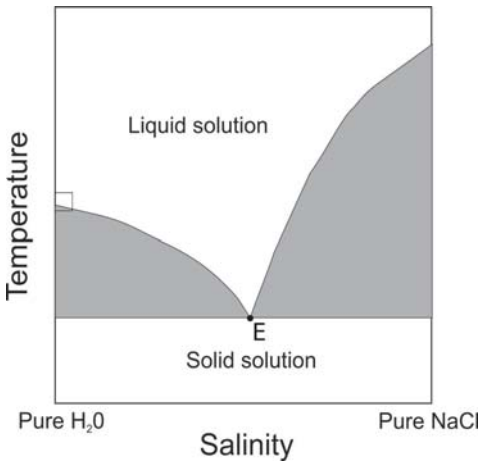

Figure 1: Phase diagram of a mixture of water and salt, at a fixed pressure.

where c_{w} and c_{i} are the specific heat capacities of water and ice, and ℓ is the specific latent heat at the freezing temperature T_{f}. The conservation of salt mass prescribes

$$M\left(S_{\mathrm{mix}}-S_{\mathrm{w}}\right)+\Delta M\left(S_{\mathrm{mix}}-S_{\mathrm{i}}\right)=0. \tag{2}$$

The changes in the seawater properties result from (1) and (2),

$$T_{\mathrm{mix}}=T_{\mathrm{w}}-\left(\frac{\Delta M}{M+\Delta M}\right)\left[\left(T_{\mathrm{w}}-T_{\mathrm{f}}\right)+\frac{\ell}{c_{\mathrm{w}}}+\frac{c_{\mathrm{i}}}{c_{\mathrm{w}}}\left(T_{\mathrm{f}}-T_{\mathrm{i}}\right)\right]<T_{\mathrm{w}}, \tag{3}$$

$$S_{\mathrm{mix}}=S_{\mathrm{w}}-\left(\frac{\Delta M}{M+\Delta M}\right)S_{\mathrm{w}}<S_{\mathrm{w}}. \tag{4}$$

As can be seen in Fig. 1, a decrease of the temperature and salinity of a liquid solution favors the coexistence of pure ice and liquid in a liquidus state. Moreover, until two phases coexist at equilibrium, the liquid properties evolve according to

$$\left(T_{\mathrm{mix}}-T_{\mathrm{w}}\right)=\left(\frac{\Delta M}{M+\Delta M}\right)\left(T_{\mathrm{eff}}-T_{\mathrm{w}}\right),\quad \left(S_{\mathrm{mix}}-S_{\mathrm{w}}\right)=\left(\frac{\Delta M}{M+\Delta M}\right)\left(S_{\mathrm{eff}}-S_{\mathrm{w}}\right), \tag{5}$$

with $S_{\mathrm{eff}}=0$ and $T_{\mathrm{eff}}=T_{\mathrm{f}}-\ell/c_{\mathrm{w}}-(c_{\mathrm{i}}/c_{\mathrm{w}})(T_{\mathrm{f}}-T_{\mathrm{i}})$, that ranges between $-85°\mathrm{C}$ to $-100°\mathrm{C}$ depending on the ice temperature. Equation (5) has a graphical interpretation on the phase diagram, and shows that during the melting, the liquid evolves along a straight line toward the point $(S_{\mathrm{eff}}, T_{\mathrm{eff}})$.

1.1.2 A closer look at the low salinity zone

Since the salinity of the eutectic points is by far larger than the actual salinity observed in the ocean, the actual zone of the phase diagram that is being used for the study of ice-ocean interaction is reduced. In the following, we focus on the framed zone of Fig. 1.

The phase diagram in this zone is sketched in Fig. 2. As previously explained, the evolution of seawater during the melting of ice corresponds on the phase diagram to evolutions

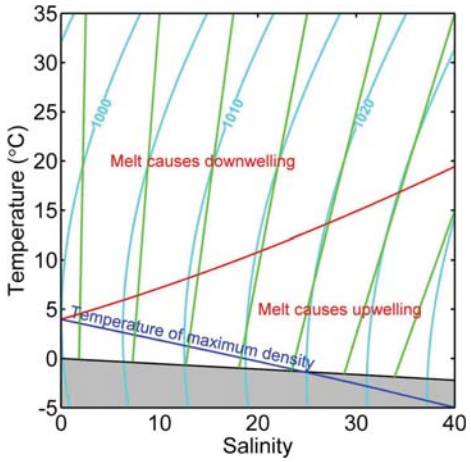

Figure 2: Phase diagram of a mixture of water and salt, at a fixed pressure and low salinities. Salinity is expressed in PSU (practical salinity unit).

along straight lines, that are plotted in green. The lines of constant density are isopycnals (in light blue) and the curve of maximal density is in dark blue).

From this information, we deduce that the melting of ice may either increase or decrease the liquid density, that is either cause downwelling or upwelling. The boundary between these two regimes is plotted in red in Fig. 2 and can be deduced from the other curves. Note that all these phase diagrams evolve with the pressure, *i.e.* with the depth.

1.1.3 Application: the "ice pump" effect

As an application of these thermodynamics properties, we describe the "ice pump" effect, sketched in Fig. 3.

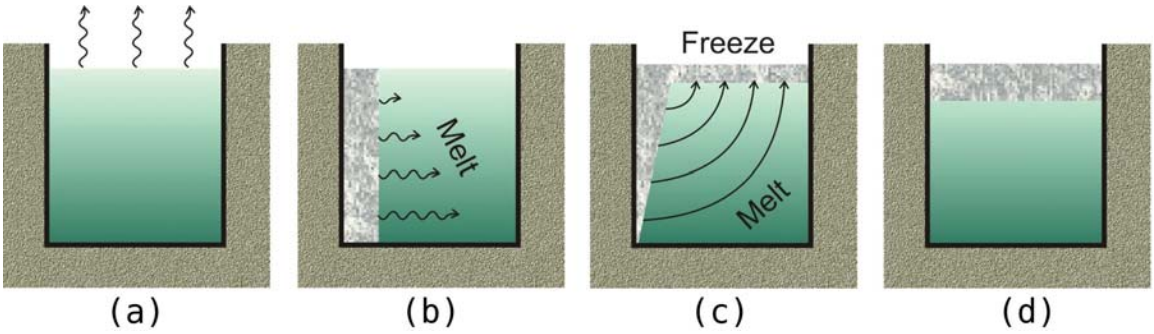

Figure 3: Sketch of the ice pump effect.

(a) We consider an insulated tank filled with water of uniform salinity and temperature, the latter being the freezing temperature at room pressure.

(b) We introduce a vertical slab of ice. Although the water at the surface is at the freezing temperature, the water at depth is not, because of the pressure dependence of the freezing temperature. This causes the ice at depth to melt, freshen, and cool the adjacent water.

(c) As seen in Fig. 2, the melting creates less dense water because of the freshening, leading to the cooled water rising. When close to the surface, the reduced freezing temperature leads the cooled water to freeze and form ice.

(d) At equilibrium, all the ice is at the surface.

1.2 The ice-ocean boundary layer

Considering the conditions required for an equilibrium between ice and seawater, we discuss the boundary layers in the ocean, in particular the ones below ice shelves. We first disregard the flow motion, then take it into account in turbulent boundary layer models.

1.2.1 Laminar boundary layers

If the water in the ocean is at rest, the situation below ice shelves could be represented by one of the sketches of Fig. 4. To connect the ocean temperature and salinity to the ones at the ice-ocean interface, where they are prescribed by the phase equilibrium, a boundary layer develops. As heat and molecular diffusion take place, this boundary layer thickens. This process may lead to convective instabilities.

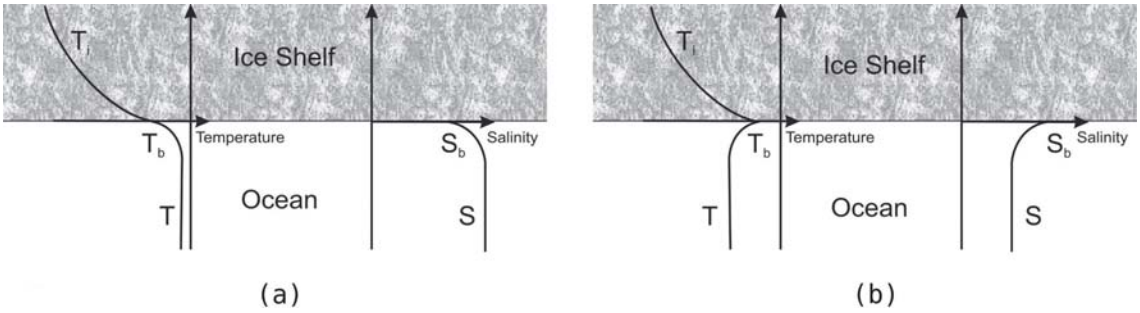

Figure 4: Temperature and salinity close to the interface.

(a) If the temperature in the ocean is larger than the one at the interface, heat is transfered to the ice shelf, that causes melting . That ablation process is unstable because of the dynamics of double diffusion: whereas the salt diffusion stabilizes the stratification, the faster heat diffusion triggers a convective instability[1]. This leads to thermohaline staircases, that are well-mixed layers separated by sharp interfaces [1]. Note that in the presence of enough shear, this differential diffusive pattern vanishes, which stabilizes the boundary (melting causes upwelling, see Fig. 2).

[1] As can be seen in Fig. 2, for ocean salinity of ~ 34.5 psu, the density evolution of water with temperature no longer presents an anomaly at low temperatures.

(b) If the temperature in the ocean is smaller than that at the interface, heat is transfered from the ice shelf to the ocean, which causes freezing. This process is unstable, because in this range of parameters freezing causes downwelling (see Fig. 2).

1.2.2 Turbulent boundary layers

Even though laminar boundary layers can be observed where the currents are weak, turbulent boundary layers are more common. They occur when there is enough shear to observe mixing in the boundary layers. They can be modeled as shown in Fig. 5, where we identify

- A surface layer, where turbulent mixing is influenced by the boundary, and an outer layer, where is it not.
- An interfacial sublayer, where the turbulence is greatly damped by viscosity. Its width, of the order of a millimeter or less, is determined by the turbulence in the outer layer. The rapid evolution of the temperature and salinity needed to match the bulk flow ones to the surface ones occur within this thin layer.

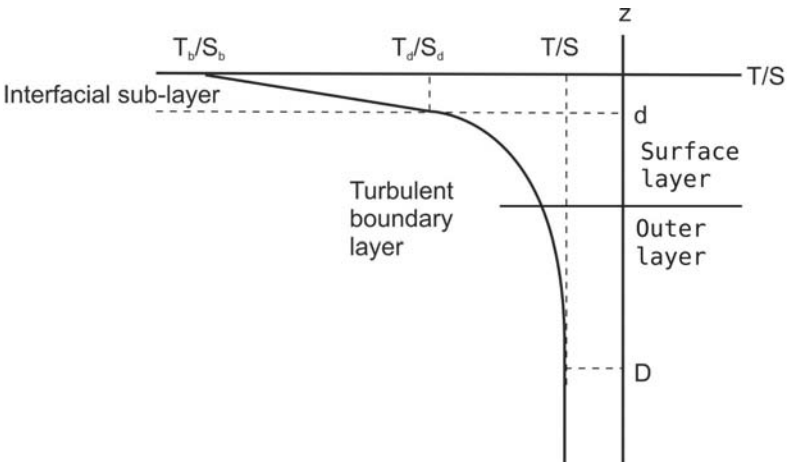

Figure 5: Turbulent boundary layer.

Whereas heat and salt fluxes, crucial to predict the dynamics of the ice shelf, can be easily worked out for a laminar boundary layer, they are much more difficult to predict in the case of a turbulent boundary layer. We present one model that describes the ice shelf evolution from these fluxes. We start by making the assumption that the freezing point at the ice-ocean interface T_b can be expressed as a linear function of salinity S_b and pressure (*i.e.* depth z_b) at this same place which we call the liquidus relationship:

$$T_\mathrm{b} = aS_\mathrm{b} + b + cz_\mathrm{b}. \tag{6}$$

We then write the energy flux balance at the ice-ocean interface,

$$\rho_\mathrm{i} a_\mathrm{b} \ell_\mathrm{i} = \rho_\mathrm{i} c_\mathrm{i} \kappa_\mathrm{i} \left(\frac{\partial T_\mathrm{i}}{\partial z} \right)_\mathrm{b} - q_\mathrm{b}^T, \tag{7}$$

where:

- $\rho_{\rm i} a_{\rm b} \ell_{\rm i}$ is the heat flux resulting from ice melting (a_b is the ablation rate, and $\ell_{\rm i}$ is the specific latent heat).
- $\rho_{\rm i} c_{\rm i} \kappa_{\rm i} \left(\frac{\partial T_{\rm i}}{\partial z}\right)_{\rm b}$ is the heat flux from the ice shelf ($\rho_{\rm i}$ is the ice shelf reference density, $c_{\rm i}$ its specific heat capacity, and $\kappa_{\rm i}$ its thermal diffusivity).
- $q_{\rm b}^T$ is the heat flux from the turbulent boundary layer that we wish to model.

We also balance the salt flux at the ice-ocean interface $q_{\rm b}^S$ with the height variation of seawater,

$$\rho_{\rm i} a_{\rm b} S_{\rm b} = -q_{\rm b}^S, \tag{8}$$

where $S_{\rm b}$ is the salinity at the ice-ocean interface. For given heat and salt fluxes, we can therefore predict the evolution of the ice shelf from this set of equations.

Theoretical predictions for these fluxes in turbulent layers can be carried out by matching solutions for an inner laminar and a turbulent logarithmic layer. The roughness of the surface can also be modeled (see, *e.g.*, [2]). *In situ* experiments suggest that simple laws apply [3], that read for the heat flux,

$$q_{\rm b}^T = \rho_{\rm w} c_{\rm w} \left(\frac{\sqrt{C_{\rm d}}}{0.006}\right) U (T_{\rm f} - T), \tag{9}$$

where w refers to the seawater, $C_{\rm d}$ is the momentum exchange coefficient, U is the velocity of the mixed layer, T is the temperature of the far-field water and $T_{\rm f}$ the freezing temperature.

1.2.3 Observations and open questions

Ice-shelf evolution As mentioned, *in situ* measurements of the heat and salt fluxes can be done based on oceanic observations of correlations between vertical velocities and temperature/salinity. In this section, we describe how direct observations of the melt rate can be performed.

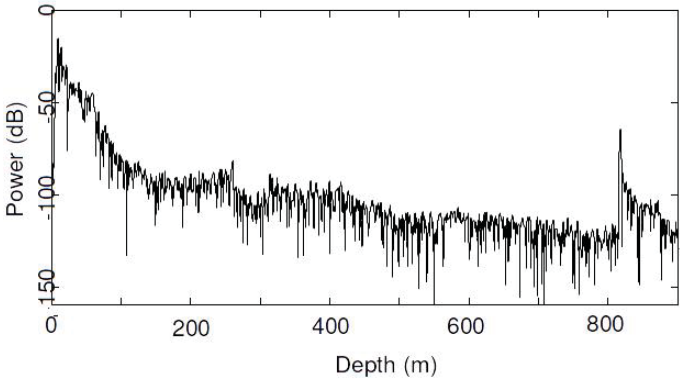

Figure 6: Power spectrum of a radar signal.

To investigate the dynamics of the basal melting, high precision radars can be used. The echo is recorded at the same place and at different times. For a given acquisition, a typical

power spectra is reported in Fig. 6; it consists of a dominant component at approximately 800m (the bottom of the ice shelf), and a multitude of other peaks, resulting from internal reflectors. The precise positions of these reflectors, randomly distributed among the ice, evolve between each acquisition because the ice shelf thickens. By looking at the displacement of the peaks in the power spectrum, it is therefore possible to track these reflectors, *i.e.* to acquire the vertical deformation field in the ice shelf, see Fig. 7.

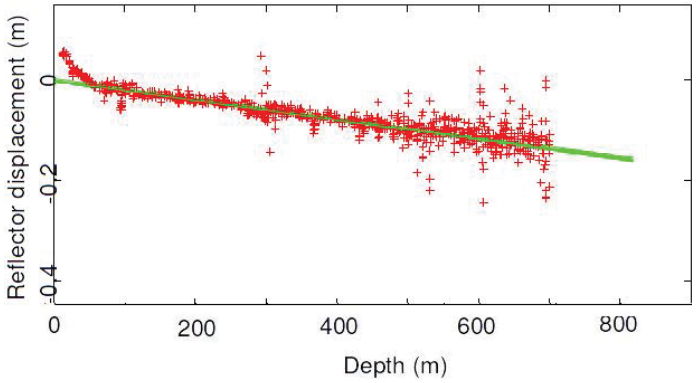

Figure 7: Evolutions of the reflectors positions.

Another possibility is to record the temperature, salinity and current below the ice shelf. This provides the information necessary to calculate the ice-ocean heat flux and the melting rate. The comparison of these two experimental methods can be used, for instance, to constrain the ice-shelf evolution models.

Vertical natural convection boundary layers The flow generated by a heated wall has been theoretically studied by Wells and Worster [4], who discuss three regimes:

1. At the smallest scales, molecular diffusion controls the heat transfer.

2. A turbulent flow develops, but initially heat transfer is controlled by the buoyancy generated at the wall.

3. As the turbulent flow grows, heat transfer is eventually controlled by the shear generated by the flow.

This problem shares similar features as the one met in the ice-ocean interactions, and may provide a model for the melting rate of vertical ice surfaces. The first regime has been sampled by early lab experiments (see, *e.g.*, [5]), the second one has been recently described [6], but the third regime has so far not been fully characterized. It remains also unclear how the processes and scales change when the ice-ocean interface becomes near-horizontal (the bottom of the ice shelf). Finally, the effect of the roughness of the interface would also need to be taken into account.

2 Buoyancy-driven Flow on Geophysical Scales

In this section, we study buoyancy-driven flows outside the boundary layer.

2.1 Scales of motion beneath an ice shelf

In the earth-fixed reference frame, the motion of seawater beneath an ice shelf obeys the Navier-Stokes equation,

$$\rho\left(\frac{\mathrm{d}\vec{v}}{\mathrm{d}t}\right) + 2\rho\vec{\Omega}\times\vec{v} = \vec{\nabla}\cdot\overset{\leftrightarrow}{\mathcal{T}} + \rho\vec{g}, \tag{10}$$

where $\vec{\Omega}$ stands for the rotation of the earth, and $\overset{\leftrightarrow}{\mathcal{T}}$ is the stress tensor (the centrifugal force has been incorporated in the pressure field). For water, the stress tensor is given by

$$\mathcal{T}_{i,j} = -P\delta_{i,j} + \rho\nu\left(\partial_i v_j + \partial_j v_i\right). \tag{11}$$

Compared to the dynamics of ice described in Lecture 1, we have retained the left-hand side of (10) and assumed water to be a Newtonian fluid.

As we shall see, depending on the part of the flow described (boundary layer, large scales, ...), some of the terms in (10) can be neglected. Typical values of the parameters for an ice shelf are given in Tab. 1.

Horizontal length	Depth	Horizontal velocity	Rotation
$L \sim 10^5$ m	$H \sim 10^2$ m	$U \sim 10^{-1}$ m $\cdot$ s^{-1}	$\Omega \sim 10^{-4}$ s^{-1}

Table 1: Scales of motion beneath an ice shelf.

Horizontal flow beneath an ice shelf For the horizontal large scales, the Rossby number (ratio of the inertial force to the Coriolis force) scales as

$$\mathrm{Ro}_L \sim \frac{U}{L\Omega} \sim 10^{-2} \ll 1, \tag{12}$$

and the inertial term can therefore be dropped. Similarly, the Reynolds number scales as

$$\mathrm{Re} \sim \frac{LU}{\nu} \sim 10^2 \gg 1, \tag{13}$$

and viscous terms remain small. Therefore, the dynamics of these large scales results from a balance between the pressure gradient and Coriolis force, which is called *geostrophic balance*. This approximation may not always be valid, for instance if the velocity is high and/or the relevant length scale is small (for instance, in or close to the boundary layer).

Structure of the Ekman layers Velocity must vanish at the solid boundaries (ice shelf base or seabed), which leads to Ekman layers. Their thickness δ can be evaluated by balancing the Coriolis force with the viscous term,

$$\rho\Omega U \sim \rho\nu\left(\frac{U}{\delta^2}\right) \Rightarrow \delta \sim \sqrt{\frac{\nu}{\Omega}} \tag{14}$$

For a typical eddy viscosity of 10^{-2}, the depth scale is $\delta \sim 10$ m. Within the Ekman layer, the velocity reduces (vanishes at the solid boundary) and its direction changes (becomes perpendicular to the geostrophic current close to the solid boundary).

Vertical motion beneath an ice shelf Since the ratio H/L is small, the flow can be described in hydrostatic balance. It turns out that gravity is balanced by the vertical pressure gradient, *i.e.* that

$$\frac{\partial P}{\partial z} \simeq -\rho g. \tag{15}$$

Therefore, we can diagnose the pressure within the ocean directly from the density distribution, as if the water were at rest.

2.2 Buoyancy-driven flow on a slope

2.2.1 Frame of reference and driving pressure gradient

We apply these approximations to the description of a flow generated by the buoyancy forcing associated with melting ice. The ice-ocean interface is assumed to be planar, but not horizontal: we note the angle α with the horizontal. This tilt allows light water to upwell along the ice shelf base.

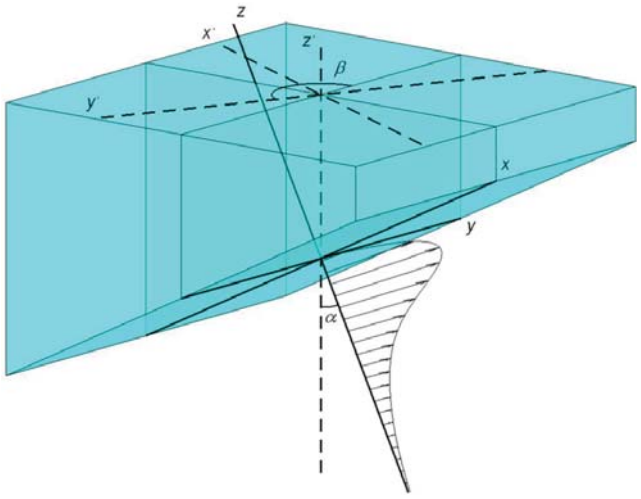

Figure 8: Coordinate system used to model the problem.

To use the same shallow water approximation as before, we consider the reference frame aligned with the boundary, see Fig. 8. We then write the Navier-Stokes equation with the

Boussinesq approximation,

$$\left(\frac{\mathrm{d}\vec{v}}{\mathrm{d}t}\right) + 2\vec{\Omega}\times\vec{v} = -\frac{1}{\rho_0}\vec{\nabla}P - \frac{\rho}{\rho_0}g\vec{k} + \vec{\nabla}\cdot \quad \nu\vec{\nabla}\cdot\vec{v} \quad , \tag{16}$$

where $\vec{k}$ is a unit vector in the local vertical direction (z' in Fig. 8) and ρ_0 is the reference density. Similarly to (15), we can apply the hydrostatic approximation along the transformed z coordinate axis, that is

$$\left(\frac{\partial P}{\partial z}\right) + \rho g\cos\alpha = 0 \Longrightarrow P(x,y,z,t) = P(x,y,\eta,t) + g\cos\alpha\int_z^\eta \rho\mathrm{d}z, \tag{17}$$

where $\eta(x,y,t)$ is the instantaneous deviation of the ice-ocean interface from its equilibrium position. We wish to compute the horizontal pressure gradient, that as mentioned before is essential for the dynamics of the large scales. For this use, we define the gradient parallel to the ice-ocean interface $\vec{\nabla}_\mathrm{H}$, and apply it to (17):

$$\vec{\nabla}_\mathrm{H}P(x,y,z,t) = \vec{\nabla}_\mathrm{H}P(x,y,\eta,t) + g\cos\alpha\left(\rho\vec{\nabla}_\mathrm{H}\eta + \int_z^\eta \vec{\nabla}_\mathrm{H}\rho\mathrm{d}z\right). \tag{18}$$

We further remove the pressure field associated with a stationary state of the ambient fluid, and assume that the ice sheet float in equilibrium with this fluid ($P(x,y,\eta,t) = 0$): this leads to the following expression for the reduced pressure gradient in the x and y direction,

$$\vec{\nabla}_\mathrm{H}P' = g\cos\alpha\left(\rho_0\vec{\nabla}_\mathrm{H}\eta + \int_z^\eta \vec{\nabla}_\mathrm{H}\rho'\mathrm{d}z\right). \tag{19}$$

2.2.2 Evolution for the layer thickness

If we consider a single active layer, depth-averaged equations sufficiently describe its dynamics. For instance, the incompressibility condition depth-averaged becomes an equation for the layer thickness $D(x,y,t)$:

$$\int_{-D}^0 \vec{\nabla}\cdot\vec{v} \quad \mathrm{d}z = \int_{-D}^0 \frac{\partial}{\partial x}v_x\mathrm{d}z + \int_{-D}^0 \frac{\partial}{\partial y}v_y\mathrm{d}z + v_z(z=0) - v_z(z=-D) = 0. \tag{20}$$

The vertical velocity $v_z(0)$ describes how the layer develops upward, *i.e.* is related to the melt rate $\dot{m}$ ($\dot{m} > 0$ if ice melts),

$$v_z(z=0) = \dot{m}. \tag{21}$$

Moreover, the kinematic evolution of the layer thickness is, with $\dot{e}$ the rate at which ambient water is entrained into the active layer,[2]

$$\left(\frac{\partial D}{\partial t}\right) + \quad \vec{v}(z=-D)\cdot\vec{\nabla}_\mathrm{H} \quad D = v_z(-D) + \dot{e}. \tag{22}$$

[2]This kinematic condition is similar to the one describing the evolution of surface elevation in the surface wave theory, where $\dot{e} = 0$.

Combining equations (20), (21) and (22), we obtain

$$\left(\frac{\partial D}{\partial t}\right) + \vec{\nabla}_{\mathrm{H}} \cdot \quad D\vec{U} \quad = \dot{m} + \dot{e}, \tag{23}$$

where $\vec{U}$ is the depth-averaged velocity, defined as

$$\vec{U} = \frac{1}{D}\int_{-D}^{0} \vec{v}\, \mathrm{d}z = U\vec{e}_x + V\vec{e}_y. \tag{24}$$

2.2.3 Depth integration of the momentum equation

The equations of motion can also be projected on the frame of reference, then depth-integrated. Note that the subscript a represents the ambient fluid and b represents the fluid at the ice-plume interface. This gives (see [7] for some details):

$$\left(\frac{\partial (DU)}{\partial t}\right) + \vec{\nabla}_{\mathrm{H}} \cdot \quad Dv_x\vec{U} \quad - \dot{e}v_{x,a} - \dot{m}v_{x,b} - \phi DV = \tag{25}$$
$$-\frac{D\bar{\rho}}{\rho} g \sin\alpha + g\cos\alpha \left[D\frac{\partial}{\partial x}\left(\eta + D\bar{\rho}\right)\right] + \vec{\nabla}_{\mathrm{H}} \cdot \left(Dv_y \vec{\nabla}_{\mathrm{H}} U\right) + \left[\left(\nu \frac{\partial v_x}{\partial z}\right)_0 - \left(\nu \frac{\partial v_x}{\partial z}\right)_{-D}\right],$$

and

$$\left(\frac{\partial (DV)}{\partial t}\right) + \vec{\nabla}_{\mathrm{H}} \cdot \quad Dv_y\vec{U} \quad - \dot{e}v_{y,a} - \dot{m}v_{y,b} + \phi DU = \tag{26}$$
$$g\cos\alpha \left[D\frac{\partial}{\partial y}\left(\eta + D\bar{\rho}\right)\right] + \vec{\nabla}_{\mathrm{H}} \cdot \left(Dv_x \vec{\nabla}_{\mathrm{H}} V\right) + \left[\left(\nu \frac{\partial v_y}{\partial z}\right)_0 - \left(\nu \frac{\partial v_y}{\partial z}\right)_{-D}\right],$$

where $\bar{\rho}$ is the depth-averaged density, subscript a refers to the ambient fluid, subscript b to the base of the ice shelf, and ϕ is the Coriolis parameter, defined as

$$\phi = 2\Omega(\cos\theta \sin\beta \sin\alpha + \sin\theta \cos\alpha). \tag{27}$$

The surface stress term can be modeled by a quadratic drag law:

$$\left(\nu \frac{\partial v_x}{\partial z}\right)_0 = -C_d |\vec{U}| U, \quad \left(\nu \frac{\partial v_y}{\partial z}\right)_0 = -C_d |\vec{U}| V. \tag{28}$$

2.2.4 Depth integration of conservation equations

Similarly, conservation equations of temperature and salinity can be derived and integrated over the depth. We get for the temperature

$$\frac{\partial (D\bar{T})}{\partial t} + \vec{\nabla}_{\mathrm{H}} \cdot \quad D\vec{U}\bar{T} \quad - \dot{m}T_b - \dot{e}T_a = \vec{\nabla}_{\mathrm{H}} \cdot \quad D\kappa_T \vec{\nabla}_{\mathrm{H}} \bar{T} \quad + \left[\left(\kappa_T \frac{\partial T}{\partial z}\right)_0 - \left(\kappa_T \frac{\partial T}{\partial z}\right)_{-D}\right], \tag{29}$$

where κ_T is the thermal diffusivity, and for the salinity

$$\frac{\partial (D\bar{S})}{\partial t} + \vec{\nabla}_{\mathrm{H}} \cdot \quad D\vec{U}\bar{S} \quad - \dot{m}S_b - \dot{e}S_a = \vec{\nabla}_{\mathrm{H}} \cdot \quad D\kappa_S \vec{\nabla}_{\mathrm{H}} \bar{S} \quad + \left[\left(\kappa_S \frac{\partial S}{\partial z}\right)_0 - \left(\kappa_S \frac{\partial S}{\partial z}\right)_{-D}\right], \tag{30}$$

where κ_S is the diffusion coefficient. Models can also be used to describe the fluxes at the ice-ocean interface, for instance

$$\left(\kappa_T \frac{\partial T}{\partial z}\right)_0 = \quad \overline{C_d}\Gamma_T U(T_b - T), \quad \left(\kappa_S \frac{\partial S}{\partial z}\right)_0 = \quad \overline{C_d}\Gamma_S U(S_b - S), \tag{31}$$

where Γ_T and Γ_S are thermal and salinity transfer parameters.

2.2.5 Simplifications

Although restricted to a single layer, this model is relatively complete and complex to solve. Some assumptions are needed to obtain an equation that describes, at a first approximation, the flow of an inclined plume. We make the following assumptions:

- the flow is in steady state
- the gradients in the cross-slope direction are negligible
- the layer is thin
- the flow is primarily baroclinic and the barotropic forcing term is unimportant
- the flow is supercritical (*i.e.* sufficiently fast compared to the speed of waves)

This leads to a simple differential equation for momentum conservation,

$$\frac{\partial (DU^2)}{\partial x} = -\frac{D\Delta\rho}{\rho_0} g \sin\alpha - C_d U^2. \tag{32}$$

2.3 A simple plume model of ice-ocean interaction

We use these simplifications to consider an even simpler problem of a buoyant plume driven by melting ice but with no outflow from underneath the glacier. In this model, ambient water melts the ice shelf at depth. It then refreezes as the plume travels upwards, like the "ice pump" example (Fig. 9). Entrainment of ambient water supplies the heat that drives melting, which modifies the buoyancy through cooling and freshening. These plumes are turbulent and entrain fluid from the surroundings, so they grow in volume as they rise. The entrainment rate is also a function of the plume velocity. Since the flow is driven by the component of gravity along the ice base, circulation and melting are sensitive to the interface slope. This process is just like a dense overflow turned upside-down.

The geometry of this problem is now simplified into one dimension where D is the depth of the plume layer, X is the along slope direction, U is the velocity of the plume in the along-slope direction, α is the angle of the slope, and T and S are the temperatures and salinities in the plume, T_i,S_i are in the ice, T_b, S_b are at the ice-ocean boundary layer, T_a, S_a are the ambient properties of the reservoir of the ocean (Fig. 10). We consider the reservoir of the ocean to be infinite in depth and to have no flow.

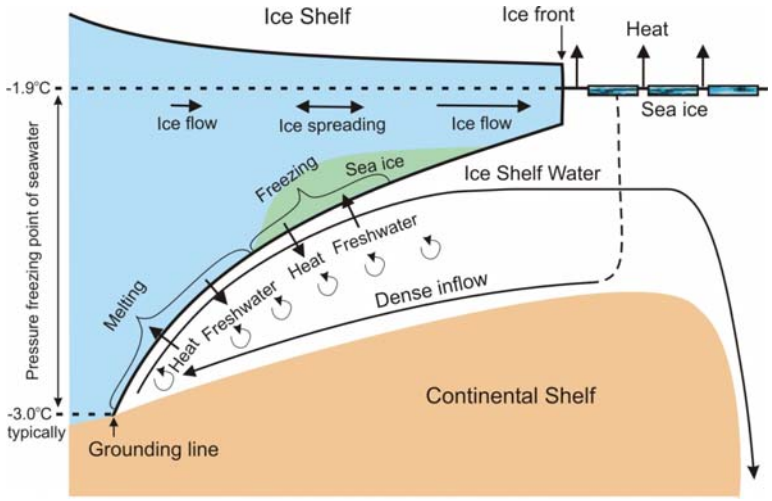

Figure 9: A schematic of a simple plume model of ice-ocean interaction. Dense water inflows at depth and melts the ice shelf, it then refreezes as the plume travels upwards.

2.3.1 Equations

We simplify the across-slope integrated equations from the previous section into 1 dimension as discussed in the previous section [8]. Conservation of mass becomes:

$$\frac{d}{dX}(DU) = \dot{e} + \dot{m} \tag{33}$$

where $\dot{e}$ is the entrainment rate and $\dot{m}$ is the melt rate. This tells us that the mass flux upward is equal to the entrainment rate plus the melt rate, because we have no other sources of mass in the system. Conservation of momentum is as derived above (Eq. 32)

$$\frac{d}{dX}(DU^2) = D\frac{\Delta\rho}{\rho_0}g\sin(\alpha) - C_d U^2 \tag{34}$$

where C_d is the drag coefficient. This tells us that the momentum imparted by the buoyancy of the plume is balanced by the drag. Conservation of heat is then written as:

$$\frac{d}{dX}(DUT) = \dot{e}T_a + \dot{m}T_b - C_d^{1/2}\Gamma_T U(T - T_b) \tag{35}$$

where Γ_T is the turbulent transfer coefficient for heat. The equation tells us that the convergence of the heat flux is equal to the amount of heat fluxed in by entrainment of ambient seawater at temperature T_a and the heat fluxed by the entrainment of boundary water, minus the turbulent transfer of heat out of the boundary layer into the plume. Conservation of salinity gives a very similar equation:

$$\frac{d}{dX}(DUS) = \dot{e}S_a + \dot{m}S_b - C_d^{1/2}\Gamma_S U(S - S_b) \tag{36}$$

where Γ_S is the turbulent transfer coefficient for salt. We take

$$\dot{e} = E_0 U\sin(\alpha) \tag{37}$$

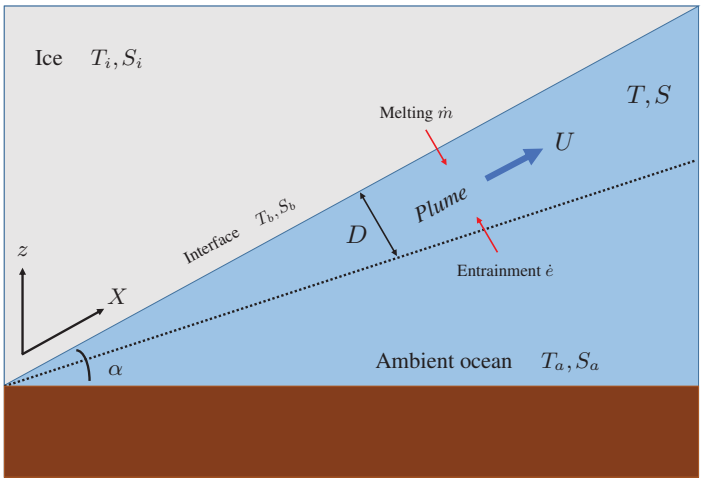

Figure 10: Geometry of the 1-dimensional problem.

where E_0 is a constant. This parameterization is related to the Richardson number of the flow, i.e. when $\alpha = 0$, then the flow cannot entrain any fluid nor travel up the slope. The equation of state is given by

$$\frac{\Delta\rho}{\rho_0} = \beta_S(S_a - S) - \beta_T(T_a - T) \tag{38}$$

The boundary conditions on the interface are given by:

$$C_d^{1/2}\Gamma_T U(T - T_b) = \dot{m}\left[\frac{L}{c} + \frac{c_i}{c}(T_b - T_i)\right] \tag{39}$$

This states that the turbulent transfer of heat at the boundary is equal to the amount of heat required to bring up the ice to its melting point and melt the ice with melting flux $\dot{m}$. The boundary condition for the salinity at the interface is:

$$C_d^{1/2}\Gamma_S U(S - S_b) = \dot{m}(S_b - S_i) \tag{40}$$

which says that the turbulent flux of salt through the boundary is balanced by a flux of salt generated by the entrainment of melt water. The final equation in our set is the liquidus relationship Eq. (6). These equations are a complete set that can be solved to understand the system.

2.3.2 Results from simplified model

First we show that the slope of the ice shelf determines how effective the buoyancy forcing is at driving the plume. Figure 11 shows the dependence of the buoyancy and velocities on the slope of the ice shelf. The plume buoyancy changes down the length of the ice shelf. The buoyancy initially increases because of the input of meltwater from the ice shelf, then decreases as freezing transfers freshwater back to the ice shelf. The steeper slopes experience

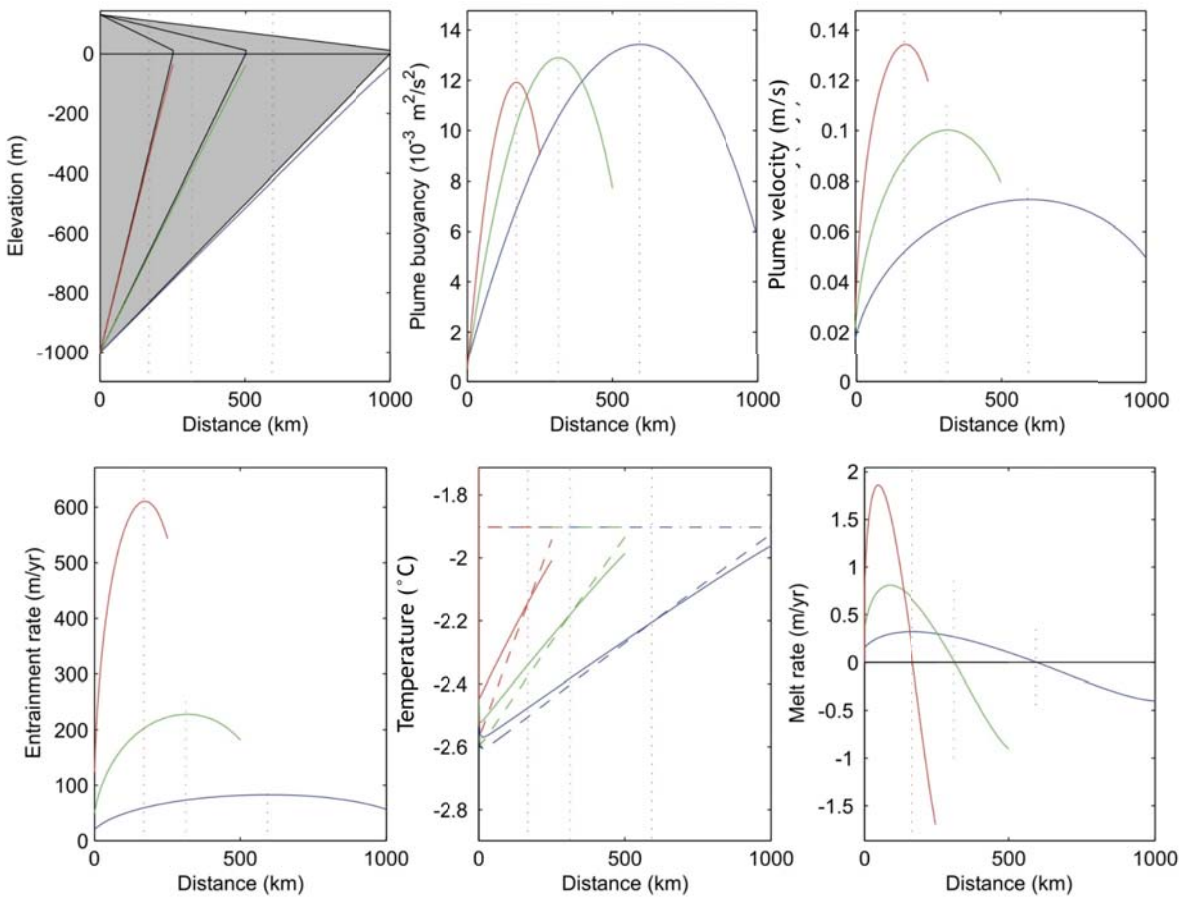

Figure 11: A figure showing the properties of plumes with different slopes. Red describes the steepest slope, green moderate, and blue shallowest. The top left panel shows the slope of the shelf, the top middle panel shows the plume buoyancy, and the plume velocity in the top right panel versus distance along the shelf (should be in m/s). The bottom left shows the entrainment rate, the bottom middle shows the temperature of the plume (solid) and the freezing temperature (dashed) and the melt rate is shown in the bottom right panel.

the maximum buoyancy at shorter distances along the shelf. The other thing to notice is that with a steeper shelf, the plume velocity is larger. The velocity also has a maximum corresponding to the location of maximum buoyancy in the plume. The plume grows in thickness as it entrains ambient seawater, which supplies the heat for melting. The buoyancy imparted by the melting drives the plume up the sloping ice shelf base. The entrainment rate is larger for a steeper slope, both because the velocity is larger, but also because α is larger (Eq. 37). We also see that the temperature begins above the freezing temperature, but depth decreases along the slope (raising the freezing temperature) and ice is melted (lowering the plume temperature), so the temperature in the plume falls below the freezing point, which leads to freezing. For a steeper slope, the melt rate is large but it quickly transitions to freezing as we move along the slope. For a shallower slope, the melt rate is lower and freezing starts much further along the slope. The heat supplied by entrainment and

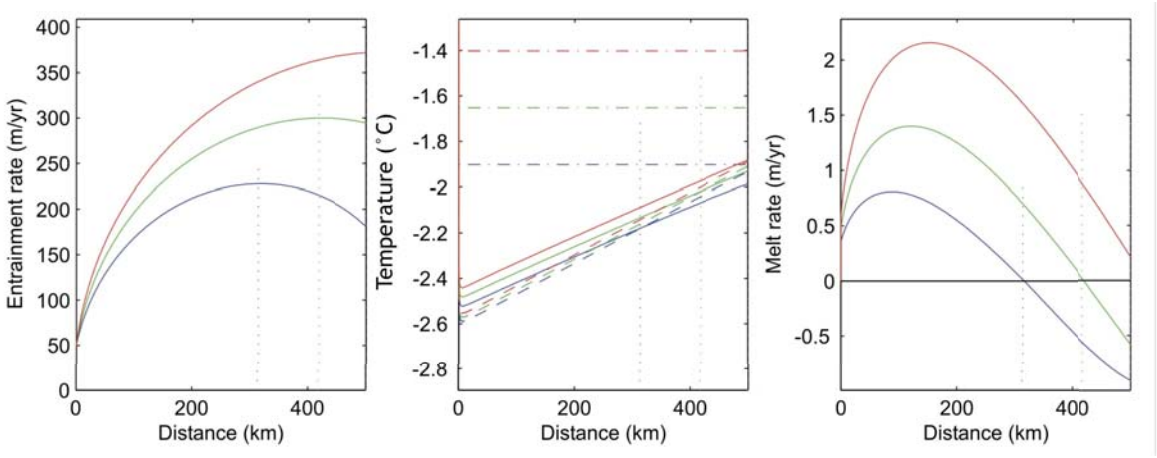

Figure 12: Entrainment rate (left), temperature (middle) and melt rate (right) for different ambient ocean temperatures. The warmest ambient ocean temperature is given in red and the coolest is blue. The dashed line gives the freezing temperature in the middle panel and the solid line gives the plume temperature.

heat lost to the ice shelf in the production of melt water are both proportional to velocity. Melting is also proportional to the temperature difference across the ice-ocean boundary layer. Entrainment warms the plume towards the ambient temperature but melting cools it towards the freezing point. As the plume grows in volume and rises towards the surface, warming by entrainment becomes less effective, leading to freezing.

Warming the ambient ocean increases the effectiveness of entrainment, so the temperature difference across the boundary layer also increases. More rapid melting implies greater buoyancy and a faster plume. Entrainment and melting both rise in response. Eventually, the zone of freezing is eliminated. In Fig. 12 we see that it takes longer for the entrainment rate to decrease in a warmer ocean and it takes longer for the freezing to begin. This begins to quantify how changing ambient ocean temperatures will affect plumes and the melting of ice shelves.

2.3.3 Melt rate scaling

In this section we will derive the temperature dependence of the melt rate. The melt rate has a non-linear dependence on the thermal driving, the difference between the ambient ocean temperature and the freezing point or $T_a - T_b$. From the thermal boundary condition in the boundary layer (Eq. 39), since the latent heat of fusion is generally much larger than the heat required to bring ice up to the melting point, this equation scales like

$$C_d^{1/2}\Gamma_T U(T - T_b) \sim \dot{m}\frac{L}{c}$$

or that

$$\dot{m} \sim U(T - T_b)$$

where T is the temperature of the plume.

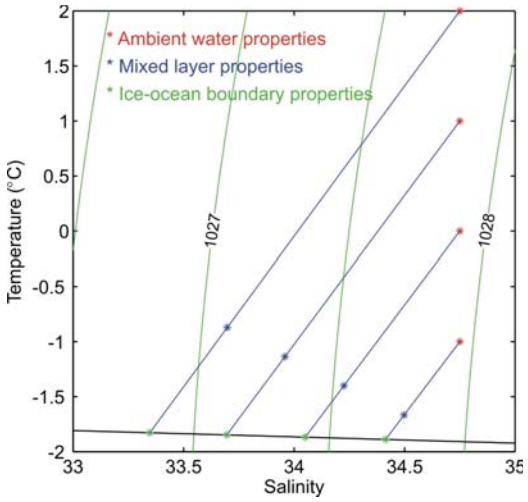

Figure 13: Mixing of the water masses.

The plume is ambient water that is modified by the addition of meltwater. Right at the ice shelf base, the water is at the freezing point. The properties of the plume water lie in between the properties of the boundary and the ambient (Fig. 13). This is evident when considering the case in steady state, where the heat entrained by mixing is equal to the heat used to melt, or

$$UE_0 \sin\theta(T_a - T) \approx UC_d^{1/2}\Gamma_T(T - T_b)$$

so that

$$\frac{(T - T_b)}{(T_a - T)} \approx \text{constant}$$

or a function of slope. Thus,

$$(T - T_b) \sim (T_a - T_b)$$

or this temperature difference scales linearly with the thermal driving. Our scaling then becomes

$$\dot{m} \sim U(T_a - T_b)$$

Now we consider the scaling for the velocity. From the momentum equation, assuming along slope changes are small, we have the scaling that

$$U^2 \sim \Delta\rho \sim (T_a - T)$$

Using the linear relationship with temperature again, we write that

$$U \sim \sqrt{T_a - T_b}$$

Finally this gives us the melt rate dependence on the temperature difference,

$$\boxed{\dot{m} \sim (T_a - T_b)^{3/2}} \tag{41}$$

That scaling is confirmed by solving the entire set of equations where we see that that the melt rate depends on $(T_a - T_b)^{3/2}$ (Fig. 14). While the relationship is always of the form given in (41), the proportionality depends on the slope of the ice-ocean interface. Steeper slopes increase the sensitivity to temperature change.

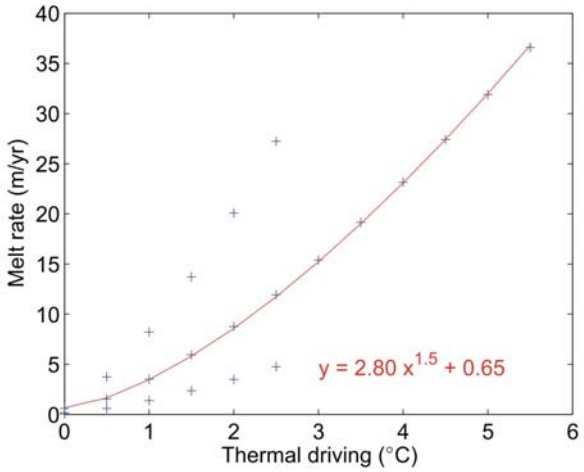

Figure 14: A figure showing the relationship between melt rate and the driving temperature.

References

[1] S. Kimura, Nicholls K. W., and Venables, E. (2015) Estimation of ice shelf melt rate in the presence of a thermohaline staircase. *J. Phys. Oceanogr.* 45, 133.

[2] A. M. Yaglom and Kader, B.A. (1974) Heat and mass transfer between a rough wall and turbulent fluid flow at high Reynolds and Péclet numbers. *J. Fluid Mech.* 62, 601.

[3] M. G. McPhee, Kottmeier, C. and Morison, J.H. (1999) Ocean heat flux in the Central Weddell Sea during winter. *J. Phys. Oceanogr.* 29, 1166.

[4] A. J. Wells and Worster, M.G. (2008) A geophysical-scale model of vertical natural convection boundary layers. *J. Fluid Mech.* 609, 111.

[5] H. E. Huppert and Turner, J.S. (1980) Ice blocks melting into a salinity gradient *J. Fluid Mech.* 100, 367.

[6] R. C. Kerr and McConnochie, C.D. (2015) Dissolution of a vertical solid surface by turbulent compositional convection. *J. Fluid Mech.* 765, 211.

[7] A. Jenkins (2016) A simple model of the ice shelf-ocean boundary layer and current. *J. Phys. Oceanogr.* 46, 1785.

[8] W. M. J. Lazeroms, Jenkins, A., Gundmundsson, G.H., and van de Wal, R.S.W. (2018) Modelling present-day basal melt rates for Antarctic ice shelves using a parametrization of buoyant meltwater plumes. *The Cryosphere* 12, 49.